

Alma Mater Studiorum Università di Bologna
Archivio istituzionale della ricerca

A proton-recoil track imaging system for fast neutrons: the RIPTIDE detector

This is the final peer-reviewed author's accepted manuscript (postprint) of the following publication:

Published Version:

A proton-recoil track imaging system for fast neutrons: the RIPTIDE detector / Console Camprini, P.; Leone, F.; Massimi, C.; Musumarra, A.; Pellegriti, M.G.; Pisanti, C.; Romano, F.; Spighi, R.; Terranova, N.; Villa, M.. - In: JOURNAL OF INSTRUMENTATION. - ISSN 1748-0221. - ELETTRONICO. - 18:01(2023), pp. C01054.1-C01054.8. [10.1088/1748-0221/18/01/C01054]

Availability:

This version is available at: <https://hdl.handle.net/11585/919372> since: 2023-03-01

Published:

DOI: <http://doi.org/10.1088/1748-0221/18/01/C01054>

Terms of use:

Some rights reserved. The terms and conditions for the reuse of this version of the manuscript are specified in the publishing policy. For all terms of use and more information see the publisher's website.

This item was downloaded from IRIS Università di Bologna (<https://cris.unibo.it/>).
When citing, please refer to the published version.

(Article begins on next page)

This is the final peer-reviewed accepted manuscript of:

Console Camprini, P., Leone, F., Massimi, C., Musumarra, A., Pellegriti, M. G., Pisanti, C., . . . Villa, M. (2023). A proton-recoil track imaging system for fast neutrons: The RIPTIDE detector

The final published version is available online at <https://dx.doi.org/10.1088/1748-0221/18/01/C01054>

Terms of use:

Some rights reserved. The terms and conditions for the reuse of this version of the manuscript are specified in the publishing policy. For all terms of use and more information see the publisher's website.

This item was downloaded from IRIS Università di Bologna (<https://cris.unibo.it/>)

When citing, please refer to the published version.

1 PREPARED FOR SUBMISSION TO JINST

2 23RD INTERNATIONAL WORKSHOP ON RADIATION IMAGING DETECTORS

3 26-30 JUNE 2022

4 RIVA DEL GARDA (TN), ITALY

5 **A proton-recoil track imaging system for fast neutrons:** 6 **the RIPTIDE detector**

7 **P. Console Camprini,^a F. Leone,^{b,c} C. Massimi,^{d,e} A. Musumarra,^{b,c} M.G. Pellegriti,^{b,c}**
8 **C. Pisanti,^e F. Romano,^{b,c} R. Spighi,^{d,e} N. Terranova^a and M. Villa^{d,e,1}**

9 ^a*Agenzia nazionale per le nuove tecnologie, l'energia e lo sviluppo economico sostenibile, Frascati, Italy*

10 ^b*Istituto Nazionale di Fisica Nucleare, Sezione di Catania, Catania, Italy*

11 ^c*Dipartimento di Fisica e Astronomia, Università di Catania, Catania, Italy*

12 ^d*Istituto Nazionale di Fisica Nucleare, Sezione di Bologna, Bologna, Italy*

13 ^e*Physics and Astronomy department, Università di Bologna, Bologna, Italy*

14 *E-mail: mauro.villa@bo.infn.it*

15 **ABSTRACT:** Fast neutron detection is often based on the neutron-proton elastic scattering reaction:
16 the ionization caused by recoil protons in a hydrogenous material constitutes the basic information
17 for the design and development of a class of neutron detectors. Although experimental techniques
18 have continuously improved, proton-recoil track imaging remains still at the frontier of n-detection
19 systems, due to the high photon sensitivity required. Several state-of-the-art approaches for neutron
20 tracking by using n-p single and double scattering – referred to as Recoil Proton Track Imaging
21 (RPTI) – can be found in the literature. So far, they have showed limits in terms of detection
22 efficiency, complexity, cost, and implementation. In order to address some of these deficiencies,
23 we propose the design of RIPTIDE, a novel recoil-proton track imaging detector in which the light
24 output produced by a fast scintillator is used to perform a complete reconstruction in space and time
25 of the interaction events. The proposed idea is viable thanks to the dramatic advances in low noise
26 and single photon counting achieved in the last decade by new scientific CMOS cameras as well
27 as pixel sensors, like Timepix or MIMOSIS. In this contribution, we report the advances on the
28 RIPTIDE concept: Geant4 Monte Carlo simulations, light collection tests as well as state-of-the-art
29 approach to image readout, processing and fast analysis.

30 **KEYWORDS:** Neutron detectors, Optical sensory systems, Particle tracking detectors, Particle iden-
31 tification methods; dE/dx detectors

32 **ARXIV EPRINT:** [2210.17431](https://arxiv.org/abs/2210.17431)

¹ corresponding author

33 Contents

34	1 Introduction	1
35	2 Proton recoil techniques and neutron tracking	1
36	3 Detector basic principles	2
37	4 Sensor chips	4
38	5 Electronics	5
39	6 Conclusions	6

40 1 Introduction

41 In the field of neutron detection, many different techniques have been developed over the years
42 to measure the yield of neutrons and possibly their energies. Interaction probability with matter
43 and detection efficiencies are a strong function of the energy and usually, for fast neutrons, the
44 detection efficiency is low. Since neutrons are neutral particles, there is not the possibility to follow
45 their track and the measurement of the neutron impinging direction is usually not possible with a
46 single detector, but relies on the knowledge of the neutron production point. Still there are several
47 interesting cases where the detection of the neutron track direction is crucial in order to distinguish
48 interesting neutrons from background signals. This is the case, for example, for solar neutrons with
49 energy $E > 1$ MeV: the only known measurement [1] done so far, from the MESSANGER probe,
50 provided no conclusive information since it was not possible to separate neutrons coming from the
51 sun from neutrons produced in secondary interactions on the probe material [2]. Nowadays this
52 field of detector research is lively advancing due to different proposals, all based on recoil proton
53 scattering. These new attempts are based on scintillating detectors or gaseous detectors enriched in
54 hydrogen where a fast neutron can have a n - p interaction, therefore it can produce a moving charge
55 in the active detector volume. The proposed detectors [3–6] suffer in general from low efficiencies
56 or the capability to determine only a single n - p interaction, thus limiting strongly their tracking
57 capability. Here we present the ideas behind a novel design [7, 8] of a neutron tracking detector,
58 called RIPTIDE (Recoil Proton Track Imaging DETector) that overcomes both limitations.

59 2 Proton recoil techniques and neutron tracking

60 Fast neutrons impinging on hydrogen rich materials like organic scintillators or organic materials
61 can give rise to n - p scattering events. For kinetic energies up to the opening of inelastic channels
62 (280 MeV), the n - p elastic cross section is dominating over or of the same size of other elastic

63 and inelastic cross sections on Carbon or Oxygen nuclei that might be present in the medium. The
 64 scattering is therefore a simple two body process with particles with almost equal masses. The
 65 energy transfer to the target proton is described simply as $E_p = E_n \cos^2 \theta$, where E_n is the impinging
 66 neutron kinetic energy, E_p is the recoil proton kinetic energy and θ is the scattering angle. Now
 67 lets suppose that a given neutron undergoes two elastic scatterings and that it is possible to measure
 68 the energies, the starting points and the directions of the two recoil protons. In these conditions
 69 it is possible to reconstruct the flight path of the neutron between the two interactions, to measure
 70 the scattering angle of the second proton and measuring its energy, it is possible to determine the
 71 neutron energy after the first scattering. By measuring direction and energy also for the first recoil
 72 proton, the final state of the first interaction is fully known. By energy and momentum conservation
 73 it is possible then to determine the energy and the direction of the impinging neutron.

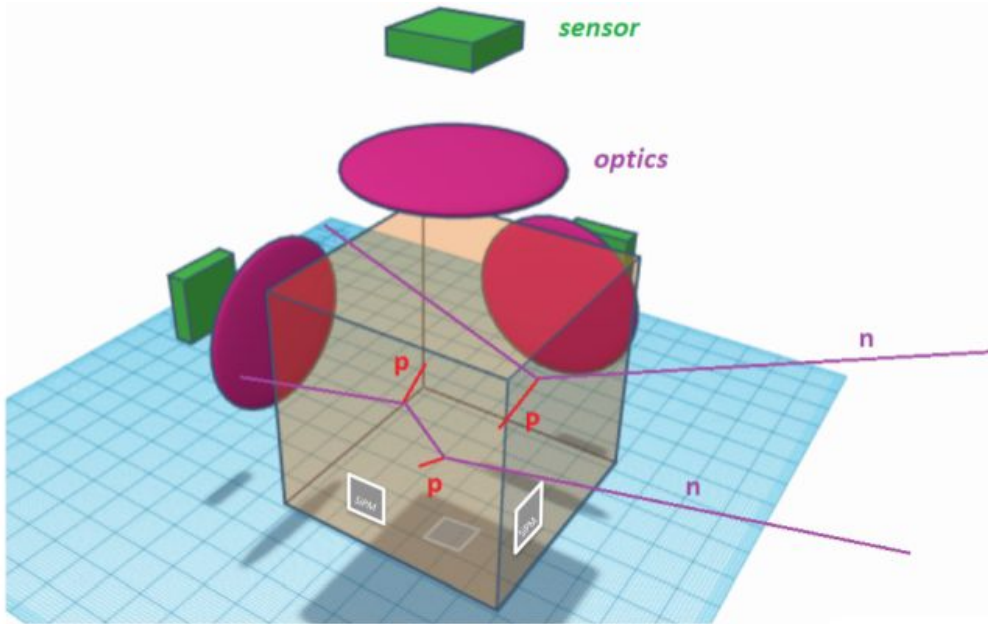


Figure 1. Minimal configuration of the RIPTIDE detector with a cube scintillator, SiPMs, lenses and optical pixel sensors. As examples, on the drawing it is possible to see a neutron interacting once and another interacting twice in the scintillator, producing recoil protons.

74 3 Detector basic principles

75 In our application we are considering for the active volume a cube of plastic scintillator with a
 76 H:C ratio of 1.1 and a typical length of $L = 6$ cm. Detectable fast neutron interactions in this
 77 volume are those on Hydrogen and, for kinetic energies up to 400 MeV, they are mainly of elastic
 78 scatterings. Recoil protons move inside the cube releasing energy in the form of scintillating light.
 79 For long enough ranges, the light production is maximal at the end of the range (Bragg peak) and
 80 it is possible to define a starting and an ending track point. The track length provides the proton
 81 energy measurement; the beginning of the track (defined as the low intensity part of the track)
 82 defines the neutron interaction point and the proton initial direction. In order to measure these

83 characteristics, we need to reconstruct how the light is produced along the track, therefore we need
 84 to observe an image of the proton track. For this reason the scintillator cube should be seen by
 85 cameras able to record the produced light and to have an actual image of the track. In order to be
 86 able to collect as much light as possible an optical system consisting of at least a lens is coupled to
 87 an imaging light detection device. Two or better three of such light detection devices are needed
 88 in order to perform the 3D reconstruction of the proton track. The scintillation cube will also be
 89 equipped with non imaging sensors (such as commercial SiPMs) to have a fast signal connected
 90 to the neutron scattering inside the cube. The whole detector is sketched in Fig.1 where, as an
 91 example, the interactions of two neutrons having a single and a double scattering are also shown.

92 Several aspects have to be accounted for in order to have a reliable and working detector. For a
 93 rough estimation of the minimal performance we consider the detection of protons with path length
 94 in the scintillator longer than 0.2 mm. This is considered the minimum length for which we'll be
 95 able to identify a track direction. This defines the minimal detectable proton energy that is 3.5 MeV.
 96 Since in typical organic scintillator the light in the cube can be evaluated as $3 \cdot 10^3$ photons per
 97 MeV of deposited energy, we'll have typically at least 10^4 photons over the entire solid angle. This
 98 light will be collected outside the cube by optical systems (lenses): necessarily we need not to rely
 99 on internal light reflection, that will be considered as a source of noise. The cube will be therefore
 100 covered by light absorbing material except for three opening (windows) from which we'll see the
 101 cube interior and for the places where SiPMs will be placed to detect direct scintillation light. Since
 102 SiPMs can be sensitive to single photons and at least 3 SiPMs will be used, there will be enough
 103 signal on each one to use their signal for triggering. In fig. 2 the probability of interaction for single
 104 and for double proton scattering are shown together with the probability of having recoil proton
 105 tracks longer than 0.2 mm.

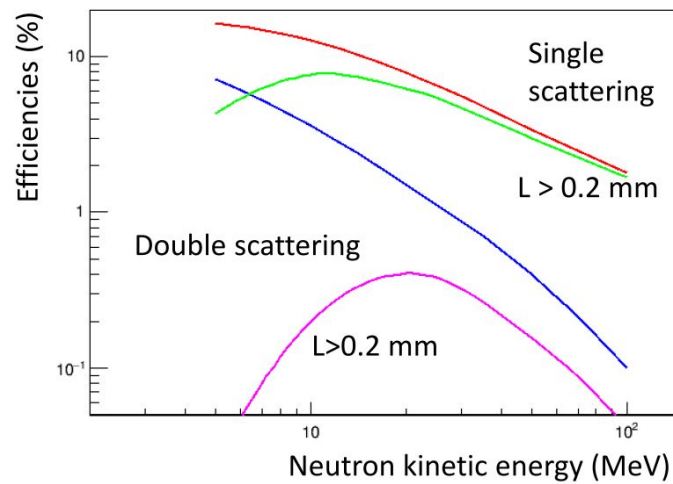


Figure 2. Probability of interaction and detection efficiency for neutrons as a function of the kinetic energy. The red line refers to single scattering into the cube; the green line refers to recoil proton ranges greater than 0.2 mm (minimum detectable). The blue line refers to double neutron scattering into the cube, while the purple line is obtained requiring that both recoil protons have a range greater than 0.2 mm.

106 For what regards the optical system, the exact position and characteristics of the lenses will

107 be defined as the optimal compromise between the need to collect as many photons as possible (a
108 large lens, placed close to the cube) and a deep field of view (long focal length). A typical lens
109 distance is in the range 5-8 cm from the cube center, which will reduce the solid angle coverage by
110 a factor of at least 20. The collected light could then be put in input to an image intensifier, made
111 by a microchannel plate or put directly to an high sensitivity imaging sensor.

112 4 Sensor chips

113 The choice of the sensor will characterize the time and spatial performances of the whole setup,
114 so it is the most critical element. The first lab studies have been performed by a small scintillator
115 coupled to a ^{241}Am alpha source coupled with a commercial camera designed for astrophotography
116 and equipped with a IMX290MM Sony CMOS sensor. The arrangement can be seen in Fig. 3.a.
117 This sensor is characterized by a large high efficiency and low noise (1 e-rms). The maximum
118 acquisition frame rate is 170 fps, much more than usually needed for astrophotography, but not
119 enough for our application. In Fig. 3.b, top part, there is a picture of the scintillator cube (6 cm
120 side length), with a plastic holding designed to host 6 SiPMs for overall signal studies. In Fig. 3.b,
121 lower part, there is a picture of the holder of the cube together with a minimal electronics for SiPM
122 powering and reading out.

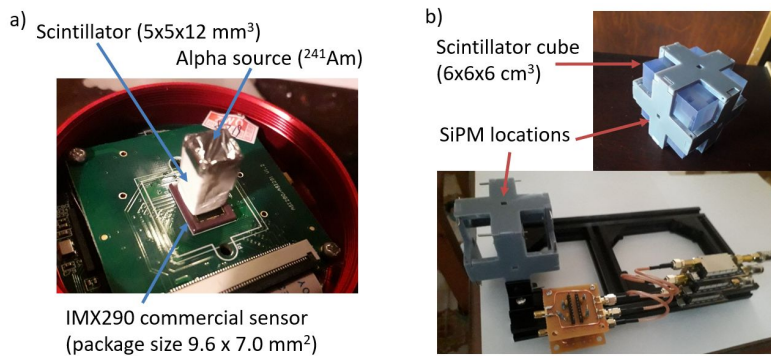


Figure 3. a) A test with a scintillator, a commercial CCD sensor and a neutron source; b) Top: the scintillator cube with the plastic holding to host the cube and the SiPM sensors; bottom: the cage and some analog electronics.

123 There are several problems related to off-the-shelf CCD sensors for our application, that makes
124 them not suitable in general. In a typical organic scintillator the light is produced in a time window
125 that can be of the order of few tens of nanosecond, up to 100 ns. Any light integration on a longer
126 time period will increase the noise in each pixel. For this reason we've searched for imaging pixel
127 sensors having high frame rates (up to few kfps) in order to be able to reduce at minimum the
128 random telegraph noise in each pixel and to be able to acquire more neutron interaction events
129 in each second. Another design requirement is related to the dead time between different frames,
130 that will constitute a source of inefficiency. This is a characteristics that is intrinsic to the readout
131 architecture of the sensor itself. At the moment we are considering two different families of sensors:
132 a) commercial high rate CCD/CMOS sensors and b) specific particle detector pixel sensors.

133 Commercial high rate CCD/CMOS sensors are designed mainly for line production checks or
134 for automotive. They are employed usually in high luminosity environments. Notwithstanding this
135 in order to collect the maximum light in each frame two interesting characteristics for our application
136 are usually present: the sensor is illuminated from the back for a maximum light collection and,
137 part of the area is used to store the charge collected from the previous exposure. This allows the
138 parallelisation of the two phases of exposure and reading, reducing the dead time at minimum. A
139 layer of microlenses helps in directing the light on the active area, enhancing the overall efficiency.
140 Due to the sparse photon countings no color filter should be used for our application. Sensors
141 matching all these requirements are for example the LUPA3000 and the LU19HS sensors developed
142 by OnSemi [9] that can reach up to 2kfps at full resolution at about 2 Mpixels. In order to improve
143 the photon statistics it is possible to use an image intensifier between the lens and the camera.
144 It is well known that Micro Channel Plates (MCP) provide suitable spatial resolution (about 10-
145 100 μm) and a large detection surface. Timing is a key feature of such a device, reaching time
146 resolution of 100-200 ps. They have been extensively used in nuclear physics, neutron, UV and
147 X-ray imaging applications since decades [10–12]. MCP implementation in RIPTIDE fulfills the
148 basic requirement of event-by-event n-tracking with sub nanosecond time resolution. Concerning
149 light detection efficiency, the use of several photocathodes can be investigated, considering that
150 state-of-the-art photocathodes for UV astronomy can achieve QE in the range 20-60% (GaN, Cs,
151 Diamond) [11]. With this approach a simple MCP or a chevron-configuration MCPs can provide
152 enhanced images on a green phosphorous screen. Images on the screen can then be recorded by a
153 high frame rate camera.

154 A complementary approach, currently under consideration, will use the image intensifier made
155 by microchannel plates, but instead of placing a phosphorous screen to receive the electrons from
156 the MCP, a particle pixel sensor could be used, as it has been done for [13]. For this configuration
157 there are several interesting chips to consider. For example, the latest version of the Timepix chip
158 [14] is a large area (7.4 cm^2) 229k pixel chip with subnanosecond timing capability and an highly
159 configurable read out. The Ultimate M28 chip [15], of the Mimosas series, is another ready solution:
160 it has about 1 Mpixels and it provides a simple hit/not hit information on each pixel. The pixel
161 matrix is read out continuously, having a rolling shutter architecture, in a fixed reading time of
162 185 μs . It has therefore a maximum full resolution frame rate of 5.4 kfps. A new sensor, called
163 MIMOSIS [16], similar to M28 for the architecture, but better for time performances is currently
164 under development for the Compressed Barionic Experiment [17]. This is a 5.4 cm^2 sensor with
165 0.7 Mpixels and a timestamping capability down to 5 μs , allowing a remarkable 200 kfps, with a
166 sparsified readout.

167 **5 Electronics**

168 The RIPTIDE detector is completed by its electronics simply sketched in fig. 4. At the core of the
169 electronics is placed a general purpose highly programmable board able to sustain high input data
170 rates. The board will be connected to the SiPMs and to the cameras. It will receive digitized signals
171 from the SiPMs that will be used to tag interesting frames. If possible the cameras will receive a
172 synchronization signal or a common clock to have the starting of the frames synchronized over the
173 different cameras. The cameras will send continuously the recorded frames to the board. The input

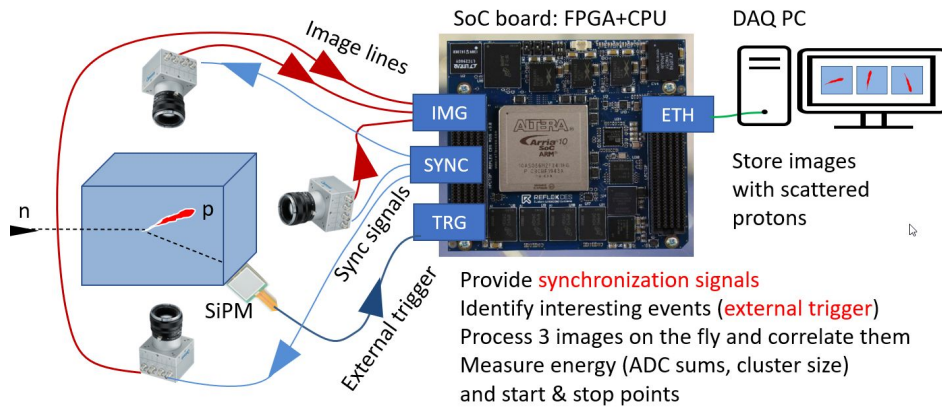


Figure 4. Schematics of the electronic connections: The scintillator cube is seen by three cameras and at least one SiPM. SiPM signal provides a trigger to tag interesting frames received from the acquisition board.

174 bandwidth for each camera/sensor can vary in a range from 1 MB/s to 10 GB/s depending on the
 175 sparsification capabilities of the sensor itself. For a typical image sensor with 1 Mpxels at 1 kfps,
 176 at least 1 GB/s input rate is needed. For sparsified readout architectures like those of M28 (max 5.4
 177 kfps) [15] or Timepix4 (single hit pixel readout) [14] input rates of 10 MB/s are usually enough in
 178 our application, aiming to have neutron interaction rates lower than 1 kHz. Since we expect that
 179 most of the frames will be empty, an on-the-fly processing of the collected images is mandatory. For
 180 this reason, an optimal choice for the electronic board is a last generation of a System-on-a-Module
 181 (SOM) board with a FPGA and an embedded ARM CPU. Simple and fast noise subtraction level
 182 and feature extraction algorithms will be applied in the FPGA to each acquired image, in order to
 183 identify images with a neutron interaction from empty ones. Moreover, events with at least two
 184 sensors having non-empty frames and/or with a fast SiPM signal in coincidence will be sent to the
 185 CPU for further processing, selection and data delivery to the final storage. The 1 Gbps ethernet
 186 ports in the SOM will be used for this purpose. Typical SOM boards based on Altera Arria 10
 187 or Xilinx Kintex 7 FPGA are well suitable for our purposes. A firmware/software code providing
 188 the basic treatment of the input data is currently being developed. From the FPGA side, it collects
 189 frames from up to 4 independent channels, it assign time-tags to them and it stores on a temporary
 190 RAM sorted by their time-tag. The RAM is handled like a circular buffer and continuously filled
 191 from one side and emptied from the other. By external SiPM signals or by feature extraction on each
 192 frame (total light collected) an internal trigger is issued and a range of interesting frames related
 193 to that trigger is identified. This information is available to the CPU side of the SOM, which is in
 194 the condition to read the shared RAM and extract the triggered frames and send them to a storage
 195 system via a 1 Gbps ethernet connection.

196 6 Conclusions

197 A new detector design providing tracking capabilities for fast neutrons using in an original way high
 198 frame rate imaging sensors has been described. The RIPTIDE detector is based on a 6 cm side cube
 199 of scintillating material that has a maximum efficiency for double neutron scattering at 20 MeV of
 200 neutron kinetic energy. The different parts of the detector have been discussed. Few options are

201 still open especially on the most critical part, the imaging sensors, that have to fulfill demanding
202 requirements: high frame rate (>1kfps), large area (>1 Mpixels) and low photon count. There are
203 interesting applications of a detector of this type that range from energy neutron measurements in
204 laboratory up to solar neutron identification and solar neutron spectroscopy in space.

205 Acknowledgments

206 The authors acknowledge the use of laboratory and computational resources from the Open Physics
207 Hub (<https://site.unibo.it/openphysicshub/en>) at the Physics and Astronomy Department in Bologna.

208 References

- 209 [1] D. J. Lawrence et al, *Detection and characterization of 0.5–8 MeV neutrons near Mercury: Evidence*
210 *for a solar origin*, *J. Geophys. Res. Space Physics* **119** (2014) 5150–5171; [10.1002/2013JA019037](https://doi.org/10.1002/2013JA019037).
- 211 [2] G. H. Share et al, *Misidentification of the source of a neutron transient detected by MESSENGER on 4*
212 *June 2011*, *J. Geophys. Res. Space Physics* **120** (2014) 1-11; [10.1002/2014JA020663](https://doi.org/10.1002/2014JA020663)
- 213 [3] J. Hu et al, *Recoil-proton track imaging as a new way for neutron spectrometry measurements*, *Sci*
214 *Rep* **8** (2018) 13363; [10.1038/s41598-018-31711-z](https://doi.org/10.1038/s41598-018-31711-z)
- 215 [4] S.M. Valle et al., *The MONDO project: a secondary neutron tracker detector for particle therapy*,
216 *Nucl. Instrum. Meth. A* **845** (2017) 556; [10.1016/j.nima.2016.05.001](https://doi.org/10.1016/j.nima.2016.05.001)
- 217 [5] M. Marafini et al., *MONDO: a neutron tracker for particle therapy secondary emission*
218 *characterisation*, *Phys. Med. Biol.* **62** (2017) 3299; [10.1088/1361-6560/aa623a](https://doi.org/10.1088/1361-6560/aa623a)
- 219 [6] J. G. Mitchell et al., *Development of the Solar Neutron TRACKing (SONTRAC) Concept*, *PoS*
220 **ICRC2021** (2021) 1250; [10.22323/1.395.1250](https://doi.org/10.22323/1.395.1250)
- 221 [7] A. Musumarra et al., *RIPTIDE: a novel recoil-proton track imaging detector for fast neutrons*, *JINST*
222 **16** (2021) C12013; [10.1088/1748-0221/16/12/C12013](https://doi.org/10.1088/1748-0221/16/12/C12013)
- 223 [8] C. Massimi et al., *“RIPTIDE” — an innovative recoil-proton track imaging detector*, *JINST* **17**
224 (2022) C09026; [10.1088/1748-0221/17/09/C09026](https://doi.org/10.1088/1748-0221/17/09/C09026)
- 225 [9] <http://www.onsemi.com>
- 226 [10] A. Pietropaolo et al., *Neutron detection techniques from μeV to GeV*, *Phys. Rep.* **875** (2020) 1;
227 [10.1016/j.physrep.2020.06.003](https://doi.org/10.1016/j.physrep.2020.06.003)
- 228 [11] A. Musumarra et al., *Measuring total reaction cross-sections at energies near the coulomb barrier by*
229 *the active target method*, *Nucl. Instrum. & Methods A* **612** (2010) 399; [10.1016/j.nima.2009.11.039](https://doi.org/10.1016/j.nima.2009.11.039)
- 230 [12] O.H.W. Siegmund et al., *Next generation microchannel plate detector technologies for UV astronomy*,
231 *Proceedings of the SPIE*, Vol. **5488** (2004) 789-800; [10.1117/12.562696](https://doi.org/10.1117/12.562696)
- 232 [13] A.S. Tremsin, J.V. Vallerga, *Rad. Meas.* **130** (2020) 106228; [10.1016/j.radmeas.2019.106228](https://doi.org/10.1016/j.radmeas.2019.106228)
- 233 [14] X. Llopart et al., *JINST* **17** (2022) C01044; [10.1088/1748-0221/17/01/C01044](https://doi.org/10.1088/1748-0221/17/01/C01044)
- 234 [15] I. Valin et al., *JINST* **7** (2012) C01102; [10.1088/1748-0221/7/01/C01102](https://doi.org/10.1088/1748-0221/7/01/C01102)
- 235 [16] A. Dorokhov et al., *The MIMOSIS pixel sensor for the CBM Micro-Vertex Detector and beyond*,
236 *Vienna Conference on Instrumentation (VCI) 2022*; [oral contribution](#)
- 237 [17] V. Klochkov et al, *The Compressed Baryonic Matter Experiment at FAIR*, *Nuclear Physics A* **1005**
238 (2021) 121945; [10.1016/j.nuclphysa.2020.121945](https://doi.org/10.1016/j.nuclphysa.2020.121945)